Thin-walled timber and FRP-timber veneer composite CEE-sections

Conference Paper · January 2015

DOI: 10.14264/uql.2016.422

CITATIONS
8

READS
389

4 authors:

Alexander Mainey
Griffith University
4 PUBLICATIONS **13** CITATIONS
SEE PROFILE

Benoit P Gilbert
Griffith University
136 PUBLICATIONS **1,597** CITATIONS
SEE PROFILE

Dilum Fernando
RMIT University
87 PUBLICATIONS **2,689** CITATIONS
SEE PROFILE

Henri Baillères
Queensland University of Technology
120 PUBLICATIONS **2,691** CITATIONS
SEE PROFILE

THIN-WALLED TIMBER AND FRP-TIMBER VENEER COMPOSITE CEE-SECTIONS

Alexander J. Mainey[1*], Benoit P. Gilbert[1], Dilum Fernando[2], Henri Bailleres[3]
[1] Griffith School of Engineering, Griffith University, Parklands Drive, Southport, QLD, Australia.
*Email: alexander.mainey@griffithuni.edu.au
[2] School of Civil Engineering, The University of Queensland, St Lucia, QLD, Australia.
[3] Salisbury Research Facility, Department of Agriculture and Fisheries, Queensland Government, 50 Evans Road, Salisbury, QLD, Australia

ABSTRACT

This paper compares the structural performance between thin-walled timber and FRP-timber composite Cee-sections. While, thin-walled composite timber structures have been proven to be efficient and ultra-light structural elements, their manufacturing is difficult and labour intensive. Significant effort and time is required to prevent the cracking of the transverse timber veneers, bent in the grain direction, when forming the cross-sectional shape. FRP-timber structures overcome this disadvantage by replacing the transverse veneers with flexible, unidirectional FRP material and only keeping the timber veneers which are bent in their natural rolling direction. The Cee-sections investigated in this study were 210 mm deep × 90 mm wide × 500 mm high and manufactured from five plies. For both section types, the three internal plies were thin (1 mm thick) softwood Hoop pine (*Araucaria cunninghamii*) veneers, orientated along the section longitudinal axis. The two outer layers, providing bending stiffness to the walls, were Hoop pine veneers (1 mm thick) for the timber sections and glass fibre reinforced plastic (0.73 mm thick) for the FRP-timber sections orientated perpendicular to the inner layers. The manufacturing process is briefly introduced in this paper. The profiles were fitted with strain gauges and tested in compression. Linear Variable Displacement Transducers also recorded the buckling along one flange. The test results are presented and discussed in this paper in regards to their structural behaviour and performance. Results showed that the use of FRP in the sections increases both the elastic local buckling load and section capacity, the latter being increased by about 24 percent. The results indicate that thin-walled FRP-timber can ultimately be used as a sustainable alternative to cold-formed steel profiles.

KEYWORDS

Ultra-light thin-walled structures, sustainable design, laminated timber structures, glass fibre reinforced plastic (GFRP).

INTRODUCTION

Increasing focus is being placed on sustainable design and construction materials resulting in many innovative approaches taken to reduce carbon emissions and increase the effectiveness of engineering structural products. One pathway is to improve the competitiveness of timber products when compared to their steel and concrete alternatives. In an attempt to create ultra-light structural elements, increase the use of timber in the construction industry and improve the profitability of the forest industry, thin-walled composite timber sections were proposed and investigated by Gilbert et al. (2014). The sections, in the form of Cee-sections with web and lip stiffeners, attempt to mimic cold-formed steel profiles through the use of a sustainably grown material. The research established that the proposed sections, when tested in compression, were able to compete with or exceed cold-formed steel products in terms of weight-to-capacity ratio.

It was noted in Gilbert et al. (2014) that delamination likely occurred within the studied specimens as a result of the experimental manufacturing techniques used. Also, the manufacturing required significant time and effort to prevent cracking of the transverse timber veneers (bent across the grain direction) when forming the cross-sectional shape. Nevertheless, damage to these veneers was still commonly observed in the studied sections. To overcome this disadvantage, this paper investigates the replacement of the transverse veneers with a flexible FRP material. Only the timber veneers which are bent in their natural rolling direction are kept, therefore creating ultra-light FRP-timber composite sections that can be manufactured faster, with less difficulty and an increase in transverse properties compared to the timber-sections.

This paper experimentally investigates the compressive performance of thin-walled timber and FRP-timber Cee-sections. An outline of the manufacturing process for both section types is given. Stub-column tests were performed and the sections were monitored throughout testing using a combination of strain gauges and transducers, enabling the structural performance and behaviour of the sections to be presented and discussed.

INVESTIGATED SECTIONS

General

Three thin-walled FRP-timber and two timber composite Cee-section specimens were manufactured in this study. The sections were manufactured in a 5-ply configuration with overall dimensions of 200 mm deep x 90 mm wide x 500 mm high, and an internal bending radius of 12 mm. The three internal timber layers for both section types were thin softwood Hoop pine (*Araucaria cunninghamii*) veneers, with a nominal thickness of 1 mm per veneer, and were layered with the grain direction orientated along the longitudinal axis of the section. For each specimen, the three internal veneers were cut from the same larger veneer sheet to maintain consistent material properties within each specimen. For the full timber sections, the external layers were cut from the same larger veneer sheet, albeit a different sheet to the internal layers, and orientated perpendicular to the inner layers. For the FRP-timber sections, the external layers (also orientated perpendicular to the inner layers) were unidirectional FRP, composed of glass fibres and polyurethane, with a combined thickness of 0.73 mm. Figure 1 outlines the specimen dimensions and grain orientation. Contrary to the sections studied in Gilbert et al. (2014), the present sections are simple Cee-sections, without web and lip stiffeners, for the purposes of manufacturing simplicity and better monitoring the compressive behaviour of the sections (see Section *Stub-column test setup*)**.** The Hoop pine veneers were glued together with resorcinol formaldehyde structural adhesive, while polyurethane was used to bond the GFRP to the timber. Polyurethane was chosen over an epoxy (those typically used in GFRP-to-concrete and GFRP-to-steel bonded joints) as it was found to provide a stronger bond to the timber.

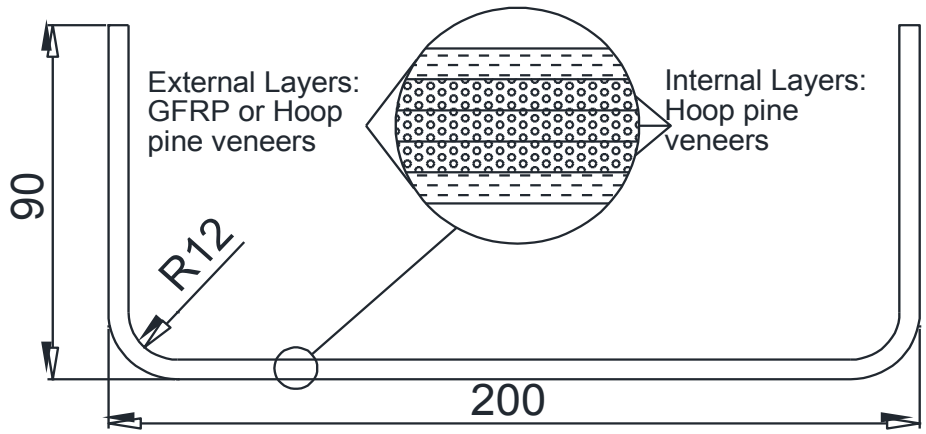

Figure 1 Dimensions and grain orientation of Cee-Sections

Manufacturing Method

Gilbert et. al. (2014) identified that delamination between the timber layers likely occurred as a result of low pressure application during the glue curing stage. In this study, the manufacturing jig was improved and the recommended glue manufacturer pressure was applied to the web while pressure on the flanges was increased through a series of heavy duty clamps. The pressure applied to the corner was also increased through the application of pressure from a thin aluminium sheet wrapped around the specimens and forced up on both sides. A schematic of the manufacturing jig used is shown in Figure 2 (a). The manufacturing process is outlined below with the steps being divided into common steps and specific steps for each section type.

Common steps

Step 1: 2.5 m x 1.2 m Hoop pine veneer sheets, 1 mm thick, were delivered and pieces were cut for specimen manufacturing and material property identification. Imperfections such as knots and cutting creases were avoided in the cut pieces.

Steps 2 to 4: Refer to the specific steps for each type of section below.

Step 5: Flanges and ends of specimen were trimmed to size.

Step 6: Specimens were placed in a climate chamber at constant temperature and relative humidity to reach equilibrium moisture content before testing as a stub column.

FRP-timber specific steps

Step 2: The three timber layers were glued around the jig (using resorcinol) and pressure was applied for 48 hours.

Step 3 The specimens were placed in a climate chamber at constant temperature and relative humidity and allowed to reach equilibrium. This ensured that the polyurethane had appropriate amounts of water within the timber to react with when applied to the specimen.

Step 4: The GFRP was then glued to the specimens around the jig (using polyurethane) with pressure being applied for 24 hours.

Note: Step 4 could be conducted at the time as step 2 in the future if the same glue is used for all surfaces.

Timber composite specific steps

Step 2: The external layers were soaked in water for 48 hours to enable their bending across the grain with minimum cracking in the timber.

Step 3: The soaked veneers were moulded into shape around the jig without the aluminium sheet, with the dry internal layers, through the use of a water steamer. This exposed the corners allowing them to dry faster. The jig was then placed in an oven at 40^{o}C for 30 minutes until the veneers could be released from the jig without losing their shape. After removal from the oven, the layers were removed from the jig, separated and held loosely in their desired shape through flange restraints in an air-conditioned room until gluing.

Step 4: All layers were glued together around the jig after they reached equilibrium moisture content. Pressure was applied for 48 hours.

A photo of the final manufactured full timber specimen, prior to trimming (Step 5) is shown in Figure 2 (b).

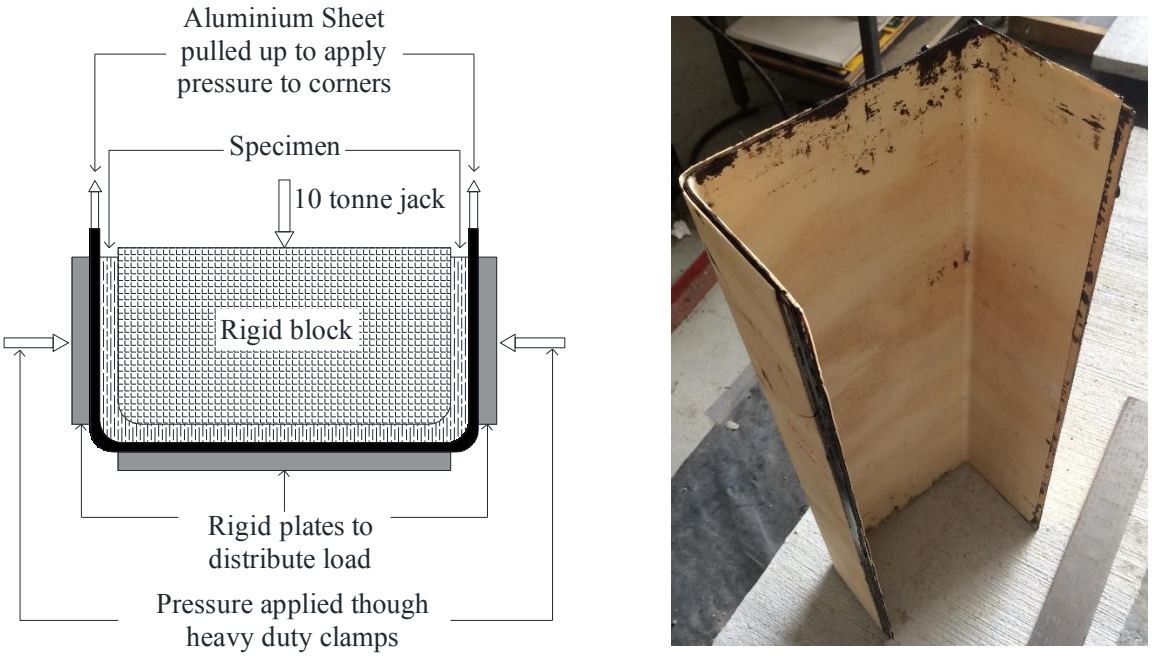

(a) (b)

Figure 2 (a) Schematic of jig used to manufacture cee-sections (b) Finished untrimmed timber section

MATERIAL TESTING

The Modulus of Elasticity (MOE) and Modulus of Rupture (MOR) parallel and perpendicular to the grain, for all timber veneer sheets constituting the cross-sections were measured.

The MOE was measured using an acoustic non-destructive method (Brancheriau, 2002). Six strips of 300 mm long and 50 mm wide, representing three strips parallel to the grain and three perpendicular to the grain, were cut from each large veneer sheet. The strips were simply-supported on two rubber bands and impacted with a hammer. A microphone recorded the vibrations which were analysed using the Beam Identification by Non-destructive Grading (BING) software (CIRAD 2015). The results are given in Table 1.

To measure the compressive MOR, 20 rectangular pieces were cut from each large timber veneer sheet and glued together to manufacture 100 mm long and 50 mm wide samples. Three samples representative of the parallel grain direction and two samples representative of the perpendicular grain direction were manufactured per veneer sheet. The samples were tested in compression till failure using a 500 kN capacity MTS universal testing machine at a stroke rate of 0.16 mm/min to achieve failure in 1-5 minutes in accordance with AS/NZS4357.2:2006. This rate also represented the same strain rate at which the Cee-sections were tested. All samples were conditioned at the same constant humidity and temperature as the timber and FRP-timber sections to reach an average oven dry moisture content of 13.9%, determined according to AS/NZS2098.1:2006. The MOR perpendicular to the grain direction was determined using a 1% strain offset as outlined in EN 408:2003. The results are summarised in Table 1.

The mechanical properties of the GFRP were also measured but are not shown in this paper.

Table 1 Mechanical properties of timber veneers used

Specimen	Parallel to grain				Perpendicular to grain			
	Average MOE (MPa)	CoV	Average MOR (MPa)	CoV	Average MOE (MPa)	CoV	Average MOR (MPa)	CoV
FRP-timber No. 1	15,671	0.100	51.2	0.200	1,186	0.014	8.2	0.108
FRP-timber No. 2	16,819	0.074	58.0	0.272	848	0.026	7.6	0.007
FRP-timber No. 3	13,288	0.093	47.3	0.253	832	0.037	9.2	0.047
Full timber No. 1 (internal layers)	16,421	0.027	51.9	0.055	1,161	0.018	9.6	0.177
Full timber No. 1 (external layers)	15,352	0.087	51.3	0.010	1,058	0.020	10.4	0.062
Full timber No. 2 (internal layers)	13,251	0.130	50.9	0.151	1,032	0.027	9.0	0.040
Full timber No. 2 (external layers)	14,304	0.126	43.4	0.196	810	0.014	7.7	0.009

STUB-COLUMN TEST SETUP

The nominally 500 mm high specimens were tested in compression using a 500 kN MTS universal testing machine. The specimens were positioned between two testing platens, as shown in Figure 3 (a). The bottom platen was fixed while the upper platen was mounted on a half sphere bearing which could rotate, providing full contact between the platen and the specimens. A 51 mm rigid steel plate was inserted between the upper platen and the specimens. The load was applied through the theoretical centroidal axis of the specimens at a stroke rate of 0.8 mm/min resulting in failure within 2.5 to 3 minutes.

The behaviour of the specimens was monitored through four Linear Variable Displacement Transducers (LVDTs) and a set of six 30 mm long strain gauges. The LVTDs were equally spaced along the bottom half of one flange, 10 mm for the edge of the flange, as shown in Figure 3 (b). The strain gauges were located in pairs on both faces of the opposite flange, 35mm from the flange edge, as well as on the outside face of the web, along its centreline, as shown in Figure 3 (b). The LVDTS aimed to capture the buckling shape of the flange, while the strain gauges aimed to capture the variation in axial and bending strain in the specimens.

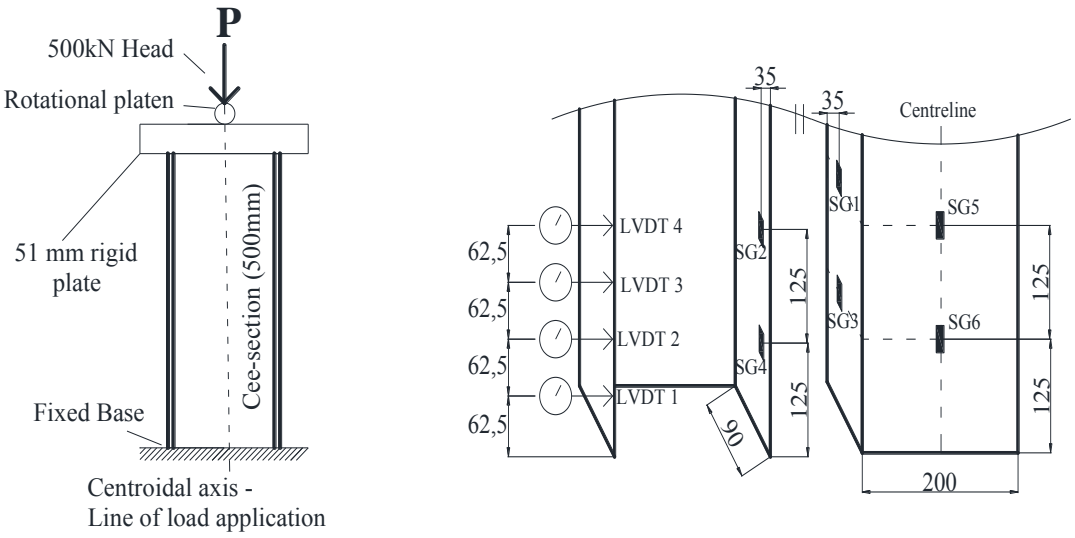

(a) (b)

Figure 3 (a) Stub-column test setup (b) LVDTs and strain gauges locations used throughout testing

STUB-COLUMN TEST RESULTS

The maximum load and apparent compressive Modulus of Rupture, $MOR_{apparent}$, of each cross-section is given in Table 2, the latter being calculated based on the measured cross-sectional area of the three internal layers that are resisting the compressive load. The efficiency of the sections, defined as the ratio between the apparent compressive MOR of the cross-section and the compressive MOR of the material (MOR_{wood}) (i.e. representing the upper bound apparent compressive strength of the cross-section and given in Table 1) is also given in Table 2.

Table 2 Stub-column test results

Specimen	Cross-sectional Area[(1)] (mm^2)	Maximum compressive load (kN)	Apparent MOR ($MOR_{apparent}$)(MPa)	Efficiency ($MOR_{apparent}$ /MOR_{wood})
FRP-timber No. 1	1,047	33.5	32.0	0.62
FRP-timber No. 2	1,029	37.3	36.2	0.62
FRP-timber No. 3	1,045	29.7	28.4	0.60
Average	--	--	***32.2***	***0.62***
Full timber No. 1	1,081	26.9	24.9	0.48
Full timber No. 2	1,015	26.6	26.2	0.52
Average	--	--	***25.6***	***0.50***

[(1)] Measured cross-sectional of internal layers only

Table 2 identifies that replacing the external timber layers with FRP increases the efficiency of the sections by 23.2% on average where the FRP-timber and full timber section's efficiency was 0.62 and 0.5 respectively. In comparison, the lipped Cee-sections (without web stiffener) investigated in Gilbert et al. (2014) had an average efficiency of 0.58. Therefore the lipped sections were 16% more efficient than the full timber sections and 7% less efficient than the FRP-timber sections investigated in this paper. For comparison, the lipped cee-sections used 36% more material than the sections investigated in this study.

Figure 4 and Figure 5 plot the recorded displacements of the four LVDTs for timber specimen No. 2 and FRP-timber specimen No. 2, respectively. These figures show that local buckling occurs at a higher applied load (67% higher) for the FRP-timber section than for the timber section, resulting in a higher ultimate load. For the FRP-timber sections, about 55% of the ultimate load was reached before local buckling occurred within the sections, against 42% for the timber sections.

The strain gauge readings for FRP-timber specimen No.1 are shown in Figure 6. The initial difference in stiffness of the strain gauge readings are due to bending of the walls from the geometric imperfections within each specimen. Elastic local buckling starts at approximately 20 kN. The axial strain (ε_{axial}) in the flanges of the

specimen, obtained by averaging the strain readings from strain gauge pairs (see Figure 3 (b)), is plotted for FRP-timber specimen No 1 and timber specimen No 2 in Figure 7 and Figure 8, respectively. These figures also identify the bending strain in the flanges, equal to half the difference of the strain readings from gauge pairs (assuming perfect bonding between plies).

The axial strain in both specimens remains linear until failure indicating that the load is evenly distributed through the entire cross-section until failure. The contribution of the bending to ultimate failure is demonstrated in Figure 8 and Figure 7 where the bending strain caused by local buckling is 290 to 330% higher than the axial strain at failure. Until 64.2% of the ultimate load for the FRP timber specimen No. 1 and 55.7% for the timber specimen No. 2, the axial stress in the flanges is greater than the bending stress, however after this point, the stress induced in the external layers is primarily due to local buckling.

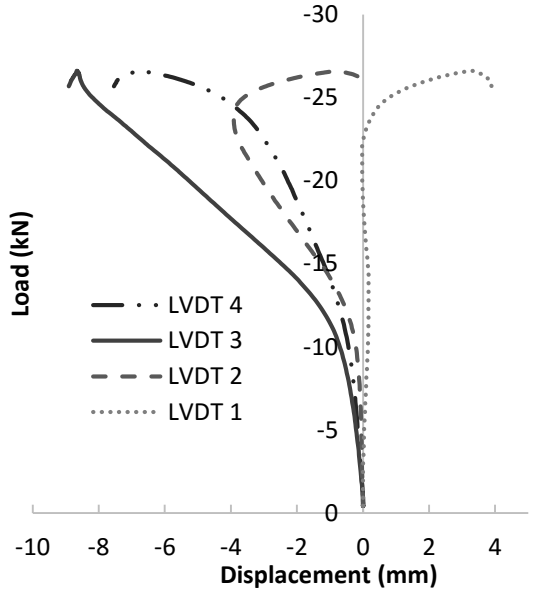

Figure 4 Displacement results from timber section No. 2

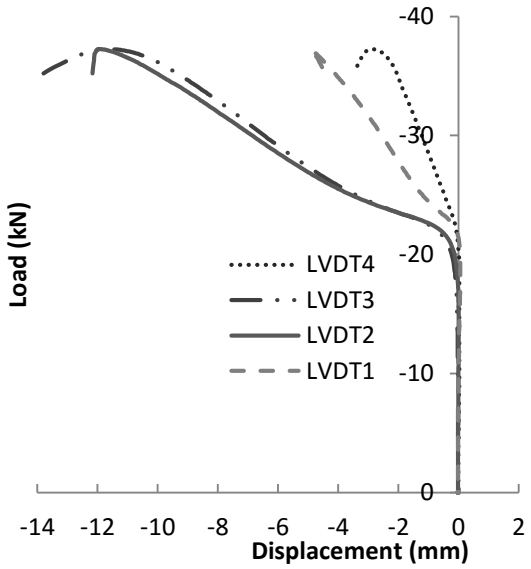

Figure 5 Displacement results from FRP-timber section No. 2

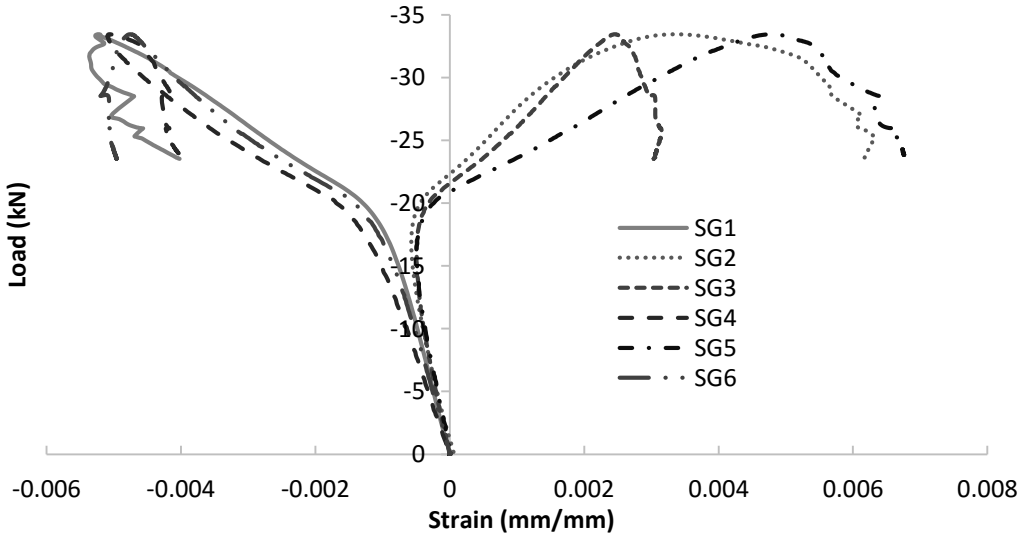

Figure 6 Strain gauge readings for FRP-timber specimen No. 1

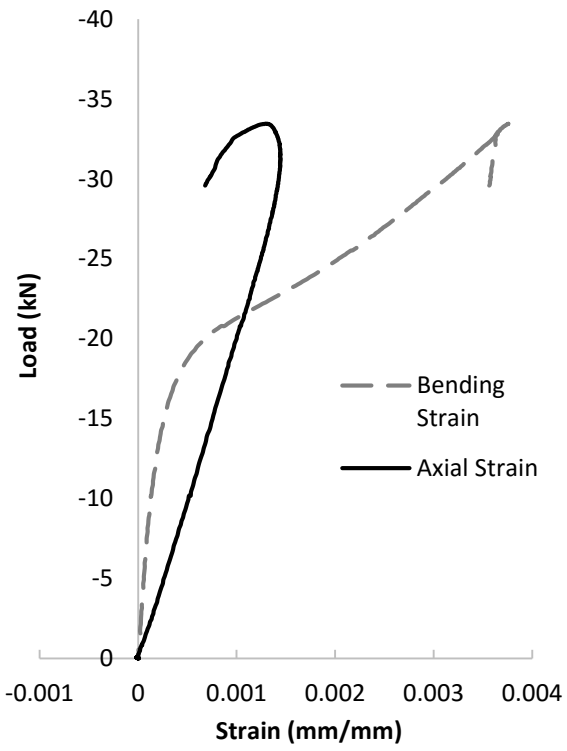

Figure 7 Axial and bending strain of FRP-timber specimen No 1 in the lower half of flange (strain gauges 3 and 4)

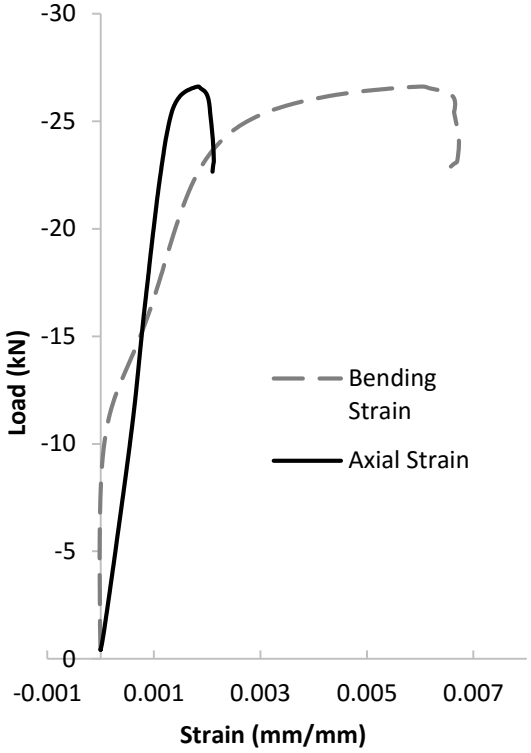

Figure 8 Axial and bending strain of timber specimen No 2 at midpoint of flange (strain gauges 1 and 2)

Two types of local buckling deformed shapes were observed for the FRP-timber sections; FRP-timber specimen No. 3 buckled asymmetrically (with limited buckling of the flange at mid-height (LVDT 4)) as shown in Figure 9 (a), while specimens No. 1 and 2 buckled symmetrically (i.e. large deflections at mid-height), as shown in Figure 9 (b). All FRP-timber sections ultimately failed in the flanges due to bending of the timber layers (see Figure 10). As failure solely occurred in the timber, the thickness of FRP was likely overdesigned and could be optimised in the future, providing it does impact of the FRP's ability to enhance the local buckling capacity of the profiles. This will in turn result in reducing the cost and weight of the specimens.

The two buckling modes discussed above were also observed in the timber sections where timber specimen No. 2 buckled asymmetrically while timber specimen No. 1 buckled symmetrically. Additionally, two distinct types of failure modes were observed for the timber sections. One flange of specimen No. 1 failed in bending at mid-height as shown in Figure 11, while the second specimen had failure ultimately occurring with tearing of the timber at the corner (see Figure 12), a likely cause of the asymmetrical buckling.

The FRP-timber and timber sections had an average measured mass of 1.40 kg and 1.22 kg per unit length, respectively. This corresponds to a weight-to-capacity ratio for the FRP-timber specimens being just 4% less that for the timber sections. However, as discussed previously, it is likely that the amount of GFRP used can be reduced and therefore the FRP-timber sections have the potential to be more efficient sections in terms of weight-to-capacity ratio than the timber ones.

(a) (b)

Figure 9 FRP-timber specimens (a) asymmetric buckling mode (Specimen No. 2) and (b) symmetric buckling mode (Specimen No. 3)

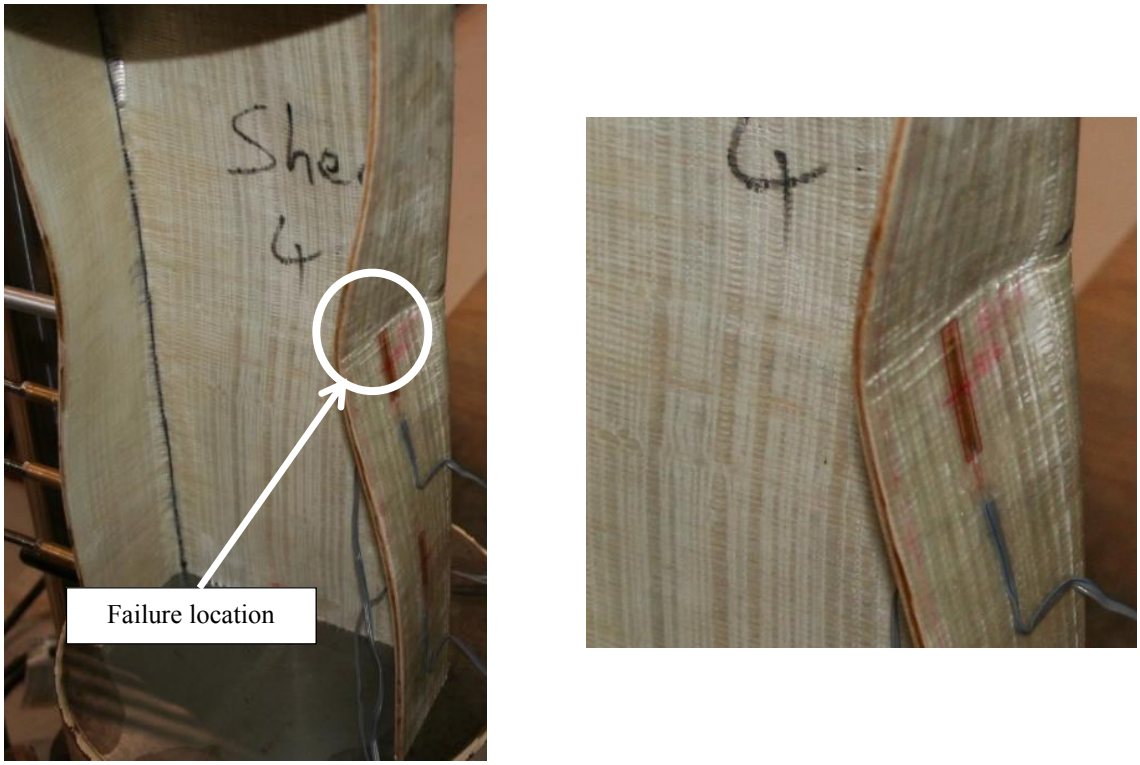

(a) (b)

Figure 10 (a) FRP-timber specimen No. 1 post ultimate failure (b) expanded view at failure location

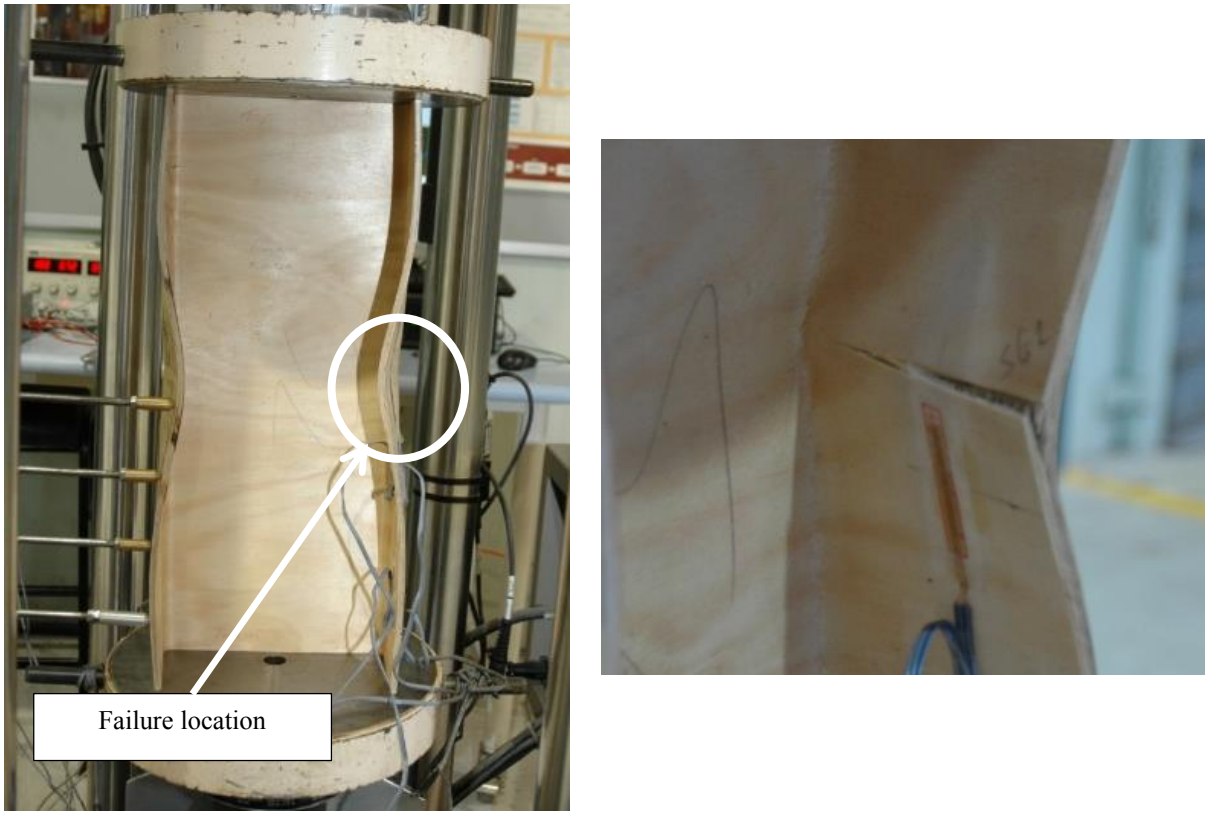

(a) (b)

Figure 11 (a) Symmetrical buckling of timber Section No. 1 and (b) bending failure of the flange

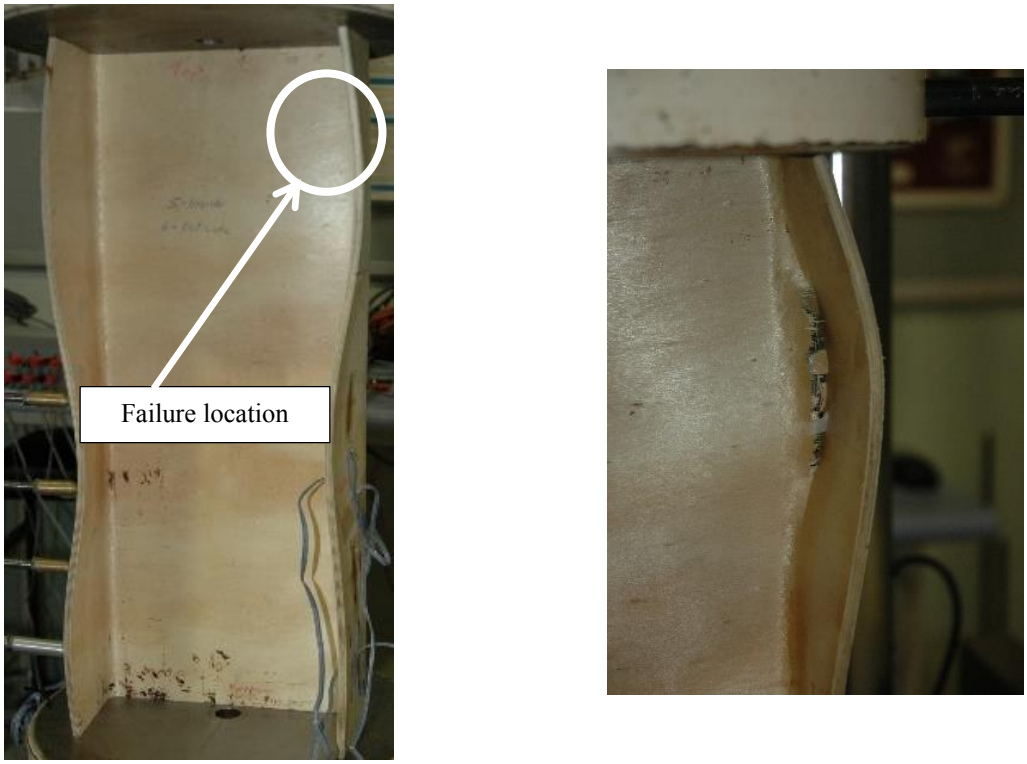

(a) (b)

Figure 12 (a) Asymmetrical buckling of timber Section No. 2 and (b) Tearing of at corner

CONCLUSION

The manufacturing issues of thin-walled timber sections encountered in Gilbert et al. (2014) were addressed in this paper and the new manufacturing process was introduced. Thin-walled FRP-timber and timber sections were manufactured and the replacement of the timber cross banded veneers with GFRP was found to significantly simplify the manufacturing process. The sections were tested in compression and the use of GFRP for the cross banded layers was shown to increase the loading efficiency of the sections by an average of 23.6%. The elastic buckling load was also increased. The two section types were comparable in performance in terms of weight-to-capacity ratio. This paper has established that the manufacture of efficient FRP-timber sections is possible and provides a pathway for sustainable and lightweight structural elements.

REFERENCES

AS/NZS 2098.1, *Methods of test for veneer and plywood*, Standards Australia, Syndey, 2006.

ASNZS 4357.2, *Structural laminated veneer lumber, Part 2: Determination of strucural properties – Test Methods,* Standards Australia, Sydney, 2006.

Brancheriau. L, Bailleres. H, "Natural vibraion analysis of clear wooden beams: a theoretical review", *Wood Science and Technology,* 36, 347-365, 2002.

CIRAD, BING® (*Beam identification by Nondestructive Grading) software*, http://www.cirad.fr/en/innovation-expertise/products-and-services/equipment-and-processes/bing-r-wood-quality-analysis-system, Accessed on 15/04/2015.

EN 408, *Timber structures*. *Structural timber and glued laminated timber*. *Determination of some physical and mechanical properties*, British Standards Inststution, London, 2003.

Gilbert, B. P., Hancock, S. B., Bailleres, H. & Hjiaj, M. 2014. Thin-walled timber structures: an investigation. *Construction and Building Materials*.